Thermal inertia and energy efficiency assessment of Direct Solar Floor system using a switching-linear model

M.H. Benzaama, L.H. Rajaoarisoa, M.C. Lekhal, S. Menhoudj, A.M. Mokhtari

Version of Record: https://www.sciencedirect.com/science/article/pii/S0306261921007686
Manuscript_f775caa9f8d6332860e9b1ec99ae1887

Thermal inertia and energy efficiency assessment of Direct Solar Floor System using a switching-linear model

M. H. Benzaama[a,*], L. H. Rajaoarisoa[b], M. C. Lekhal[c], S. Menhoudj[d], A. M. Mokhtari[d]

[a] *COMUE Normandie University - ESITC-Caen Research Lab, 1 Rue Pierre et Marie Curie 14610 Epron, France*
[b] *IMT Lille Douai, Institut Mines-Télécom, Univ. Lille, Centre for Digital Systems, F-59000 Lille, France*
[c] *MSME Laboratoire, UMR-8208 CNRS, Université Gustave Eiffel, 77420, Marne-la-Vallée, France*
[d] *LMST Laboratory, University of Sciences and Technology, Mohamed Boudiaf, Oran, Algeria*

Abstract

This study presents a case study of a room equipped with a Direct Solar Floor (DSF) in order to predict the true thermal and energy behaviour. DSF operation during the night by thermal inertia is a complex phenomenon, and its relative impact is proven to be influenced by many factors including the solar radiation and the thermal insulation of the slab. However, current physical models don't show this relationship efficiently. This paper will demonstrate by adopting switching linear models that this relationship can be described formally with a numerical model. In fact, the simulation models developed in literature are represented in a very simplified method and cannot be used for a detailed analysis of thermal operations of DSF. The present study aims to reduce the knowledge gap and resolve the limitations such as (i) a realistic explanation of the thermal behaviour of direct solar floor, (ii) identify the heating mode by thermal inertia in a quick and easy way and (iii) estimate the heating time by thermal inertia for a long period, which can later estimate the gain in energy consumption bring. The switching model has detected three operation modes of the Direct Solar Floor, one of which corresponds to the moment of heating by thermal inertia. The model can also evaluate the duration and the energy provided by the thermal inertia. As a result, it has been estimated at 310hours and 18.6kWh for a test period of 1110hours, which corresponds to an average of 3.58hours per day.

Keywords: Direct Solar Floor (DSF); Thermal inertia; Thermal behaviour, Energy efficiency, Operating modes, Heating, Switching model, PWARX model.

1. Introduction

In Algeria, the building sector has become the most energy-intensive sector, accounting for more than 42% of the final energy consumption that reaches 30 million Tep. After the transport sector, it represents 30% of the balance of carbon dioxide emissions and produces an emission of 25.3 million TeCO2 [1]. Thus, to reduce buildings energy consumption, it is necessary to develop new energy systems in order to limit greenhouse gas emissions and the effects of climate change. The challenge is today to improve the comfort of indoor environments by reducing energy consumption regarding heating needs. One of the solutions is to integrate renewable energy systems in the building. Controlling energy consumption and ecological problems have highlighted the use of renewable energies. The integration of renewable energy systems (e.g. solar thermal) in the buildings has been the subject of several experimental and numerical types of research. Most of them focus on the study and evaluation of the building energy performance for the heating needs. One of the applications of low-temperature solar energy is the direct solar floor heating (DSF) system. In this system, the solar energy for heating is transferred directly by the anti-freeze heat transfer fluid from the solar collectors to a slab without an intermediate heat exchanger.

The DSF is not sufficiently developed in the literature because its performance depends on solar deposit to ensure thermal comfort, unlike the solar heat pump system. The parametrization of three essential parts in the installation is important to ensure a good functioning of the system: Solar collector (Type, size, orientation, geographical location), control (over the solar collector temperature, the indoor air temperature and the floor temperature) and thickness of the slab.

The application of DSF has been presented in the literature for several climate conditions by conducting experimental and numerical studies for the purpose of optimization. The study elaborated by Papillon in [16] showed that the use of a slab with a significant thickness of 30 cm was not necessary and that a slab with a reduced thickness of 15 cm could replace it while having considerable energy performances of the underfloor heating system. In Algeria, Kazeoui et al. in [8] studied the energy saving of building equipped with DSF. They save huge energy due to the reduction of heating load after the installation of the direct solar floor, which resulted in a significant reduction of conventional air conditioning use. In

*I am corresponding author
Email addresses: mohammed-hichem.benzaama@esitc-caen.fr (M. H. Benzaama), lala.rajaoarisoa@imt-lille-douai.fr (L. H. Rajaoarisoa), mohammed-cherif.lekhal@u-pem.fr (M. C. Lekhal), smenhoudj@yahoo.fr (S. Menhoudj), am_mokhtari@yahoo.fr (A. M. Mokhtari)

[13], authors studied by experimental fashion the energy performance of the DSF and the energy-saving provided in terms of the heating needs of a room. They showed that the solar coverage provided by the DSF amounts to more than 67% for a capture ratio of 0.2.

In [20], authors conducted a numerical (TRNSYS tools), experimental and economic study on the energy performance of a solar floor heating system for a traditional bathroom (Hammam) in Marrakech city in Morocco. The Hammam was controlled by measuring air temperature and humidity as well as IR thermography. They showed that the feasibility of the solar heating floor system in the Hammam reduces annual heating energy consumption by at least 72% compared to electric and gas heating systems. On the other hand, Shilei Lu et al. in [11] conducted an experimental and numerical study (TRNSYS tools) in Ninghe, China about the introduction of phase change material (PCM) in the DSF. The authors showed that if the ambient temperature is at 20°C, the experimental building can save 5.85% energy consumption compared to the building without PCM.

During the winter season, thermal performance and economic study are investigated in [6] for a solar heating system energetic performance for different climates in Iran (Tabriz, Tehran, and Kish island). The authors carried out a numerical simulation using design builder software. The findings indicate that the annual fuel consumption decreases by 125.39, 303.58, and 1.41MWh respectively for Tehran, Tabriz, and Kish island when they associate building with a solar collector.

In [23], the authors studied and analyzed the thermal performance of a DSF in cold areas (Jinan, China) and developed a model under MATLAB Simulink. The operating parameters (solar radiation intensity, collector area, collector tilt angle, storage tank volume, tube spacing) influencing the system performance were studied. The simulation results obtained can be used as a reference for the design of a DSF heating system for cold regions in China.

It is investigated in [12] the thermal performance of two solar heating technologies for buildings in Tunisian climates. The first system is DSF and the second is a Solar Heating System coupled with an integrated active layer in the wall. The authors carried out an experimental study and numerical simulation using TRNSYS 16 software. The findings indicate that the use of a Solar Heating System with an integrated active layer in the floor presented a great potential with a solar fraction of about 78%.

Several models were used to simulate the thermal behaviour of DSF. The majority of the models presented in the literature are physical models implemented on TRNSYS tools. An accurate thermal model is essential to improve forecasting and the evaluation of energy performance. Three types of models can be distinguished:

- White-box models which are based on physical knowledge of the system and thermal balance equations. These are often obtained through energy simulation software such as TRNSYS;
- Black-box models which use only measured input/output data and statistical estimation methods such as ANN models;
- Grey-box models, a mix of the first two categories above. They use input/output data as well as some a priori knowledge on the system.

However, each technique has its advantages and weakness. One of our motivation is to discuss these points. In [3], it is presented a comparative study between these different models. The conclusion was:

- For white-box models such as TRNSYS tools: (i) the use of the white-box model often requires a great setup and computation time. (ii) It also involves numbers of inputs to define the model, such as the composition of the building envelope and the operating parameters (solar radiation intensity, collector area, collector tilt angle, storage tank volume, tube spacing). In some studies, it is difficult, if not impossible, to recover this input.
- For black-box models like ANN models, thermal performance prediction based on available data, preferably a large set of data, with genetic and machine learning method. Besides, it is difficult to understand the physical phenomena using this type of models and the thermal behaviour change (operations) related to the climatic conditions, occupants behaviour, the set-point temperature, etc.
- For grey-box models, this type of models is useful for introducing physical meaning into data-driven models, especially when different thermal behaviours need to be explained.

Thermal inertia affects how a direct solar floor responds to changes in external and internal conditions, creating a phase shift (time lag) between energy absorption and release. Thus, we can observe a few moments when the water has been introduced into the tube and when the surface temperature changes. This conduction phenomenon depends on the thickness of the slab and the thermophysical characteristics of the materials. Moreover, the thermal inertia of buildings is a complex phenomenon, which is not always well understood by specialists, especially in direct solar floor applications. Most numerical studies have been performed using white-box models (physical models) to learn building thermal behaviour. The researchers have often argued that thermal mass is beneficial for maintaining indoor thermal comfort and reducing energy demand [19].

Besides, the DSF with a large amount of thermal mass needs more time to reach the heating setpoint temperature, particularly for intermittent solar collector use. That might cause thermal discomfort for occupants and result in increased energy consumption. On the other hand, the thermal inertia of DSF used during the night create a complex phenomenon. Its relative impact is influenced by many factors, for instance, the solar radiation of the studied site or the thermal insulation of

the slab [4]. To our best knowledge, this paper is the only experimental study on the effect of thermal inertia on the direct solar floor. However, several studies investigate the impact of the thermal inertia of the slab heating (typical installation without coupling with a flat solar collector) on the comfort and energy consumption of the building as [10]. The results reported such a system to be able to deliver good thermal comfort.

Kattan et al.(2012) in [7] modelled a radiant heating floor through one-dimensional heat flow coupled to a room represented by a single node. With this model, they can study two office rooms thermal behaviour under Lebanese climate and demonstrated a 26% peak power reduction potential due to the thermal mass utilization. Other new studies exist in the literature. They propose to develop physical models that take into account the effect of the pipe wall's thermal inertia [22]. Herein, the authors presented the impact of including thermal inertia in the model on the accuracy of this one. They evaluated the phase shift between the temperature considering the pipe wall's thermal inertia and without considering it. The phase shift time can be up to 8.9min. As can be seen, the literature is not unanimous on the relevance of direct solar floor thermal mass activation. We conclude that estimating the effect of thermal inertia on building energy consumption and thermal comfort is not always self-evident. Furthermore, no model allows yet identifying the moment and the duration of the heating by the thermal inertia.

Motivated by these last results we introduce in this paper a novel idea using a switching grey box model called piecewise ARX model (PWARX) to identify the time and duration of heating by the thermal inertia of DSF. This study shows the different DSF operation modes with a comparison with TRNSYS tools (White box). The research questions corresponding to the objectives are:

- What is the thermal performance of the DSF for the mediterranean climate (Oran city)?
- The PWARX model should be able to explain the true thermal and energy behaviours of the building by identifying the usage scenarios?
- The PWARX model should be able to identify the moment and duration of heat release by the thermal inertia of the slab?
- What is the difference between TRNSYS and PWARX models?

1.1. Paper contribution

The models mentioned above and for most of the solar floor heating models, presented in the various studies reported in the literature, use a simplified representation of heat transfers. Their computation is realized thanks to its electrical analogy, which assumes the average temperature of the heat carrier fluid is the mean between the inlet and the outlet ones. This approach uses a physics-based formulation to describe the dynamic behaviour of heat conduction, storage and release. It allows to study and compare many building variants without the limitations related to measurement setups. However, modelling accurately the effect of thermal inertia requires solving the differential-algebraic equations for time-dependent heat transport [15; 21]. The analytical approaches could provide an exact solution, but one of the important limitations is that they lend themselves for simplified cases and boundary conditions [15; 21].

Some analytical approaches add Fourier analysis to describe the temperature profile as a sum of sinusoidal components, but this still does not reflect the real complexity of time-varying outdoor temperature and incident solar radiation [15; 21]. The significant limitation of these approaches is that they lack to integrate the complexity of real-life buildings, in which multiple heat fluxes such as solar gain are present [15; 21]. Numerous literature can be found on radiant systems including calculation methods [5], operative temperatures for comfort [18], cooling capacities [14] and modelling [24]. Besides, detecting the moment of heating and the calculation of the energy provided by thermal inertia is not yet done. It should be mentioned that almost all the network models reported in the literature can predict the change in indoor air temperature only as a function of switching the pump ON and OFF. Using these models, we can't quantify the contribution of the thermal inertia of the slab for a long test period, which is considered an important parameter for this type of installation. Furthermore, the physical approaches presented above have limitations in predicting the delay time of temperature propagations. It is particularly true when the investigation is for a long-time period. As a result, the diagnosis is difficult for an engineer. Moreover, no model can yet evaluate the heating time by thermal inertia for the DSF system.

The limitations mentioned above do indeed indicate a lack of knowledge that needs to be addressed. Surmounting these limitations will then allow us to provide an accurate dimensioning of the solar heating floor for different climates. To this end, the main contributions will be structured along three (3) aspects considered essential:

1. propose a new data driven model that can provide a realistic explanation of the thermal behaviour of direct solar floor.
2. identify the heating mode by thermal inertia in a quick and easy way
3. estimate the heating time by thermal inertia for a long period, which can later estimate the gain in consumption bring.

For a long test period, we will show in this paper that the operating modes could influence the thermal behaviour of the indoor air, especially at night. The effect of thermal inertia is surprising unexpectedly during the night due to the decrease of the indoor and outdoor temperature. For this case, we will show that the switching model (PWARX) can detect in which period the thermal inertia has requested to cover the heating needs, and in which case the use of supply heating is necessary. This method could be considered as a "new" contribution to the literature.

2. Methodology

In line with what is already proposed in the literature, we have developed a new conceptual framework that summarises and visualises our research methodology. The conceptual study plan of our work consists of three main parts, as illustrated in Figure 1. Each of them is composed of several steps. These will be explained in detail in the following sections. However, they can be summarised as follows:

- *Stage one*: in this step, an experimental test bench is developed. A direct solar floor is installed in an experimental cell equipped with several measurement sensors (temperature, humidity, etc.). An experimental data collection and analysis is carried out in this stage. This part is detailed in Section 2.1.1.

- *Stage two*: the decision to use the PWARX model is mainly due to the capacity of this approach to detect the change in thermal behaviour due to a different mode of operation such as weather conditions, control system, etc. For data-based models, two separate data sets are required: the training data set and the validation data set. The training data set is used to train the model, to find the parameters such that a good fit is obtained. In the case of the PWARX model employed here, the training data set is used to find the number of sub-models (number of operating modes). The set of validation data are utilized to investigate the precision of the estimated model. This part is detailed in Section 2.1.4.

- *Stage three*: simulate the direct solar floor using transient system simulation modelling (TRNSYS tool). In this step, the TRNSYS components corresponding to the solar thermal sensor, experimental cell, and meteorological file are used. The real thermo-physical parameters of the wall composition, the solar collector, and the control system used in the experimental cell are taken into account.

2.1. Direct solar floor thermal modelling

2.1.1. Fundamental principle

Direct solar floor (DSF) is a system consisting of: a solar thermal collector connected directly to a floor heating system as shown in Figure 2. Solar radiation is collected by the solar thermal collector to heat the circulating fluid using a pump. The fluid has then flowed into the floor heating which, in turn, transmits the heat brought by the fluid and diffuses it inside the building.

The type of solar collector considered in this work is a flat glass collector with a surface area of $4.6m^2$ with an inclination of 45^o and facing South (Figure 3). The collector can supply the floor heating for heating needs. The hydraulic circuit is made of PER (cross-linked polyethylene) in two loops with a diameter of 18 mm. The spacing between pipes at floor level is equal to 20 cm. The pipes are laid on a welded mesh laid on the insulation, embedded in a 10 cm thick slab (see Figure 3).

The circulation of fluid is done by means of a control system (Figure 4). The value of the control signal is chosen as a function of the difference between the upper and lower temperatures Th (Higher input temperature) and Tl (Lower input temperature). They are compared with two dead-band temperature differences DTh (Higher dead-band = 5^oC) and DTl (Lower dead-band = 2^oC).

2.1.2. Thermal inertia of the Direct Solar Floor

The thermal inertia of the DSF depends on its absorption, which is mainly related to the thickness of the slab active in heat storage. The system operation consists of (i) the absorption of thermal energy by the solar collector, (ii) the storage of this energy by the slab and (iii) its restitution as heat to the ambient environment.

Figure 5 demonstrates the energy management of the DSF, from absorption and storage to restitution of this energy by the floor heating. Herein, a wave signal represents the incident solar energy, and the energy stored and released by the floor heating is illustrated by a sinusoidal signal. As shown in the graph, the energy storage starts sometime after the rise of the solar energy and the heat release (end of storage) begins where the solar energy ends. From absorption to restitution, a thermal phase shift occurs due to the thermal inertia of the slab. This phase shift is evaluated between the two maxima (daily time difference) of the solar energy incident on the solar collector surface and the energy stored in the slab at the moment of its restitution. Also, the energy lost is calculated as the difference between the maximum incident solar energy and the one stored in the slab just before its release.

2.1.3. Transient System Simulation modelling

As mentioned in the previous paragraphs, one of the best-known tools in building thermal simulation research is the TRNSYS (Transient System Simulation Tool) software. It has developed by the University of Madison (USA) and coded in Fortran. It has a modular architecture and presents a few libraries of components that can be linked together.

So, based on the fundamental principle and parameters defined before, we can simulate different system under this software. It will be used mainly to reproduce the energy performances of the whole system. The test cell is modelled, in our case, by using Type 56 (Multizone Building Modeling) via TRNBuild. This component provides a more efficient way to calculate the interaction between two or more zones by solving the coupled differential equations.

The solar thermal collector is modelled using type 73. This component reproduces the thermal performance of a theoretical flat plate collector based on the Hottel-Whillier steady-state model. The circulation of fluids inside the solar network (collector) is ensured by type 3b, which models the operation of a hydraulic pump. The solar collector has a surface area of 4.6 m2 with a south-facing orientation and a slope of 45^o. The energy received by the solar collector surface is modelled

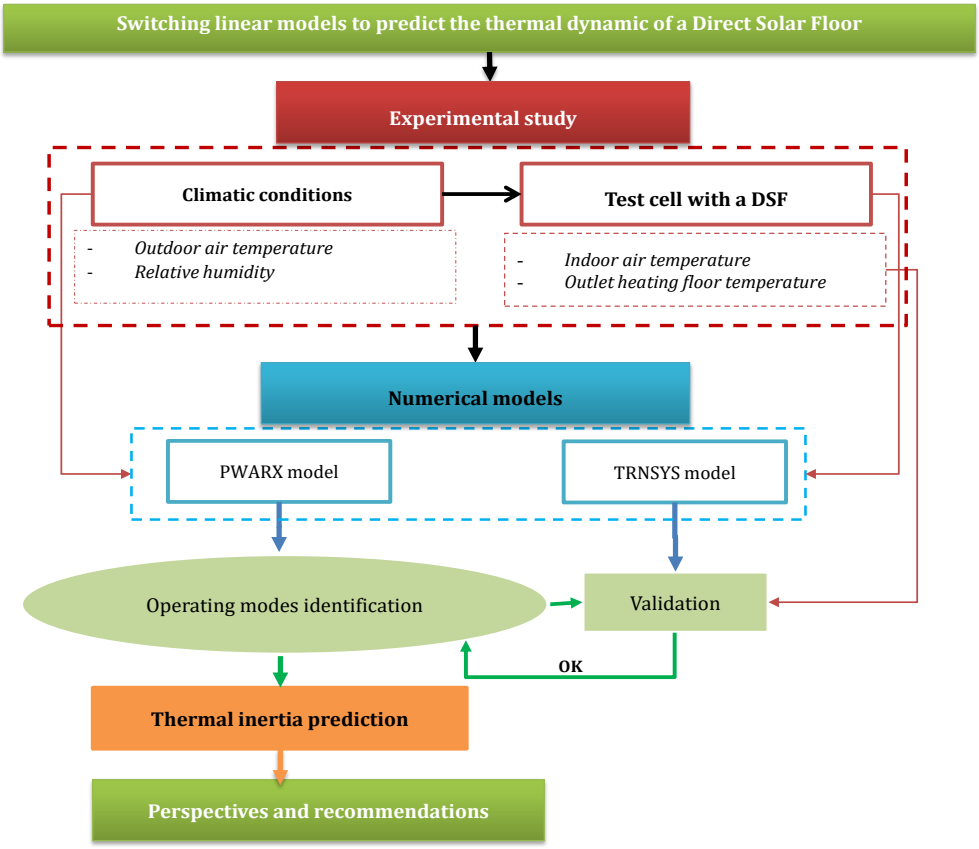

Figure 1: Conceptual study plan

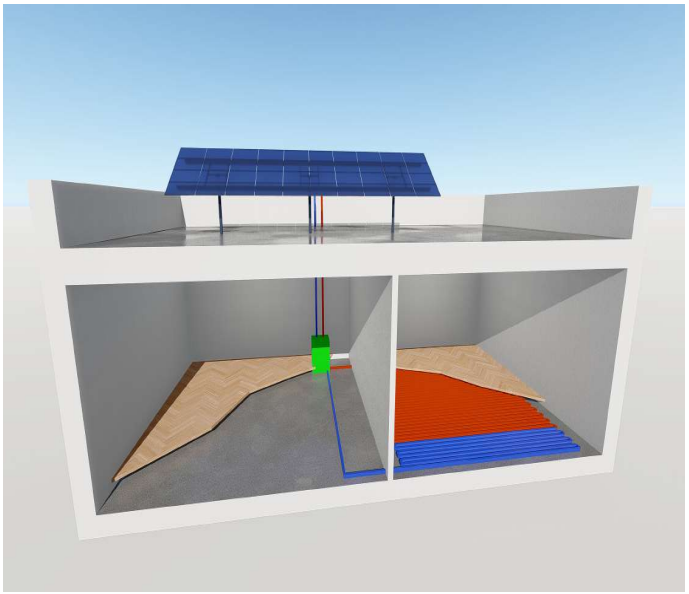

Figure 2: Direct Solar Floor coupled to the experimental cell

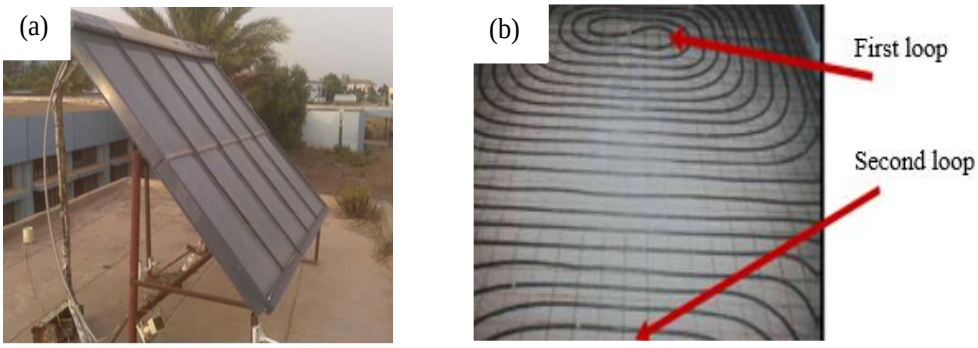

Figure 3: (a) Thermal solar collector, (b) Floor heating hydraulic circuit configuration[2].

Figure 4: Regulation and heat transfer module [2]

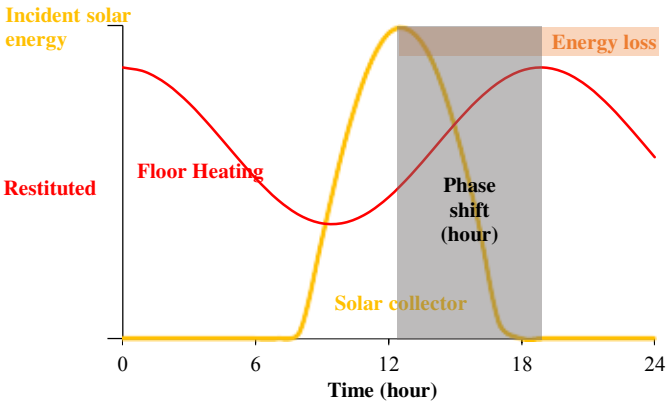

Figure 5: Energy behavior of the DSF on an incident solar energy magnitude: phase shift and lost energy.

according to the Hottel-Whillier equation:

$$Q_u = \frac{A}{N_S} \sum_{j=1}^{N_S} F_{R,j}\Big[I_T(\tau\alpha) - U_{L,j}(T_{w,j} - T_a)\Big] \qquad (1)$$

where A is the total collector array aperture (m^2), N_S is the number of identical collectors in series, I_T is the global radiation incident on the solar collector (kJ/hm^2), $\tau\alpha$ is the product of the cover transmittance and the absorber absorptance, U_L is the thermal loss coefficient (W/m^2K), T_w is the inlet temperature of the fluid to the collector (^oC), T_a is the ambient air

temperature (^oC) and F_R is the overall collector heat removal efficiency factor which is calculated by:

$$F_{R,j} = \frac{N_S \dot{m}_w C_{pw}}{A U_{L,j}} \Big[1 - exp(\frac{-F' U_{L,j} A}{N_S \dot{m}_w C_{pw}})\Big] \quad (2)$$

where $\dot{m}_w$ is the mass flow rate of the water flowing through the pipe (kg/h), C_{pw} is the specific heat of the water (kJ/kgK) and F' is the collector efficiency factor which is given according to the following equation:

$$F' = \frac{R_{absorber-Ambiance}}{R_{Fluid-ambiance}} \quad (3)$$

Finally, the DSF system model is developed based on the types and techniques offered by the TRNSYS software. The main component of the DSF TRNSYS-model is a solar thermal collector, which is modelled using the type 73. The type 3b ensures the fluid circulation inside the solar network and the Type 2b manages the differential temperature regulation. As a result, one can see on Figure 6 the developed DSF model.

Thus we can see that the development of the model under TRNSYS can be tedious as the designer has to input all the parameters defining the building systems. He must also take into account the assumptions of simplifying the heat exchange gradient by a standard temperature approach. Furthermore, he will not be able to check the errors in the surfaces and volumes entered in the program.

To overcome these limitations, we propose in the sequel to model the thermal dynamics of the DSF by a data-driven approach, data collected from the system under study. Such a method should help us to estimate and explain the thermal behaviour of the whole system (building and equipment) efficiently under its environment specifications. The following paragraph will present the ins and outs of the technique.

2.1.4. Switched and piecewise affine models

To predict the thermal behaviour of building heated by the DSF system we adopt in this paper switched affine models. This kind of models is defined by a set of linear/affine models connected by switches, indexed by an additional variable with a discrete value, called a discrete state. Models for which the discrete state could determine by a polyhedral partition of the input/output domain. They are also called piecewise affine models (Figure 7). This class of models are interesting for modelling nonlinear systems. Indeed, it can describe them by considering a linear relationship between the input/output pair.

So, let us consider firstly a linear ARX model, using an input/output (y, u) representation, writing as follows:

$$y(t) = -a_1 y(t-1) - \cdots - a_{n_a} y(t-n_a) + b_1 u(t-1) + \cdots + b_{n_b} u(t-n_b) + e(t) \quad (4)$$

where n_a and n_b are the model order, a_i and b_i are the model coefficients, $e(t) \in \mathbb{R}^{n_e}$ is a white noise process and n_e is the noise system order. In other terms, the ARX model can be defined by the following relations:

$$A(z)y(t) = B(z)u(t) + e(t) \quad (5)$$

with

$$A(z) = 1 + a_1 z^{-1} + \cdots + a_{n_a} z^{-n_a} \quad (6)$$

and

$$B(z) = b_1 z^{-1} + \cdots + b_{n_b} z^{-n_b} \quad (7)$$

where z is a backward shift operator.

So, for available input measurements, we can estimate the output $(\hat{y})$ at each time t by the ARX model as follows:

$$\hat{y}(t) = B(z)u(t) + e(t) + (1 - A(z))y(t). \quad (8)$$

Finally, in compact form the estimate of the output can be writing as:

$$\hat{y}(t) = \varphi^T(t)\theta \quad (9)$$

with

$$\varphi(t) = [y(t-1) \cdots y(t-n_a) \quad u(t-1) \cdots u(t-n_b)]^T \quad (10)$$

and

$$\theta = [a_1 \cdots a_{n_a} \; b_1 \cdots b_{n_b}]^T. \quad (11)$$

In these equations, φ represents the regression vector and θ the parameter vector. In the context of the design of a direct solar floor thermal model, y generally represents the indoor temperature, and u represents the measured factors that influence the temperature evolution.

So, the general structure of the switched ARX model can be written as:

$$y(t) = f(\varphi(t)) + e(t) \quad (12)$$

with f as a piecewise affine map of the following form:

$$f(\varphi(t)) = \begin{cases} \theta_1^T \bar{\varphi}(t) & \text{if } \sigma(t) = 1 \\ \quad \vdots & \\ \theta_s^T \bar{\varphi}(t) & \text{if } \sigma(t) = s, \end{cases} \quad (13)$$

where $\bar{\varphi} = \begin{bmatrix} \varphi^T & 1 \end{bmatrix}^T$ is the extended regression vector. $\sigma(t)$ is the switching rule defined by:

$$\sigma(t) = i \text{ iff } \varphi(t) \in \Re_i, \text{ for } i = 1, \cdots, s; \quad (14)$$

and $\{\theta_i\}_{i=1}^s$ are the parameter vectors that define the sub models. $\{\Re_i\}_{i=1}^s$ represent a complete partition of the region $\Re \subset \mathbb{R}^n$, with $n = n_e n_a + (n_b + 1)$, and each region is a convex polyhedron with:

$$\Re_i = \{\varphi \in \mathbb{R}^n : H_i \bar{\varphi} \preceq \mathbf{0}\} \quad (15)$$

where H_i and $\mathbf{0}$ are respectively a matrix of appropriate dimensions defining the limit of the region partitioning the set of regression vector and the null vector.

As shown in the synopsis in Figure 8, the proposed approach is composed of three steps which are:

- initialization : definition of all parameters required to run the algorithm. Such as initial number of operating modes, system orders, convergence rate,
- data re-affectation and model estimation : computation of each hyper-parameter according to each operating mode identified,

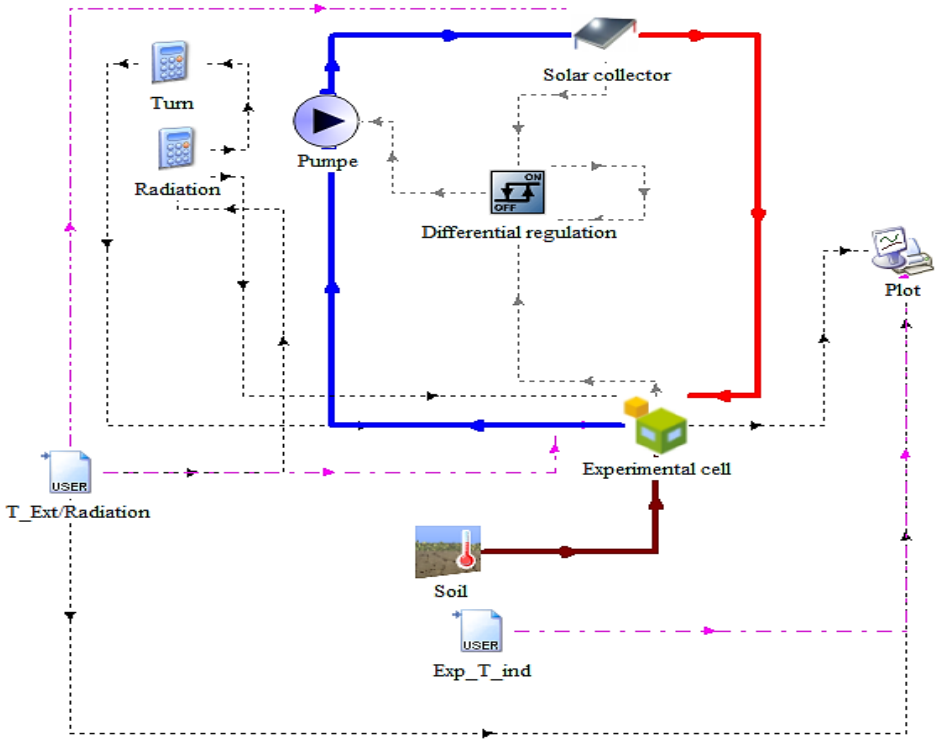

Figure 6: Simulation flow chart in TRNSYS space

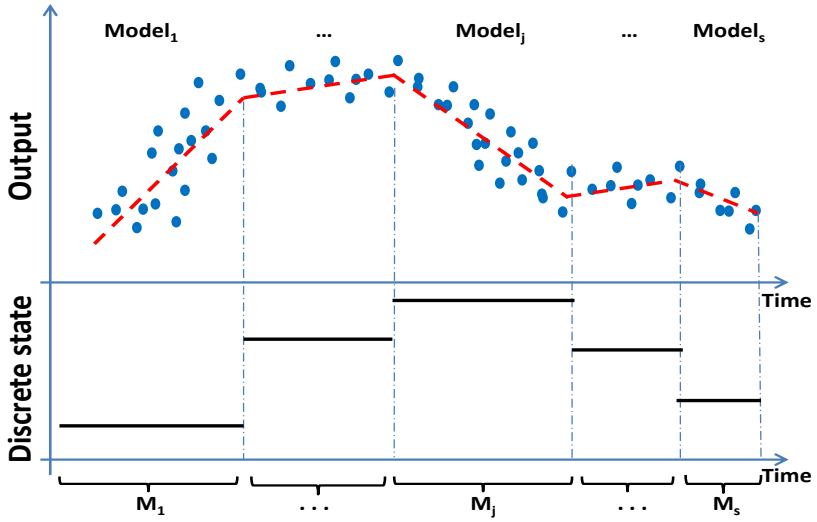

Figure 7: Switched piecewise linear models.

- convergence test : verification if hyper-parameters computed are optimal.

Accordingly, the algorithm has as inputs the input-output data $\{y(i), \varphi(i)\}_{i=1}^{N}$ and the number maximal of samples K to consider for the creation of a class and as output the sub-models s, classes $\{\mathscr{C}_i\}_{i=1}^{s}$ and parameter vectors $\{\hat{\theta}_i\}_{i=1}^{s}$. At initialization, the data will be used to create N_i classes and then they are reassigned by iterative process until the stop criterion. Indeed, it will be necessary to stop the data reassignment procedure. Reader can refer to [3] for further information about the parameter identification and estimation for this class of models.

2.2. *Model validation*

To quantify the performance of each model, let us consider, among any others, the FIT criterion value. This criterion represents the similarity between the measured output y and the output ŷ predicted by the model. It is given by the following equation:

$$FIT = (1 - \frac{||\hat{y} - y||}{||y - \bar{y}||}) \times 100\% \tag{16}$$

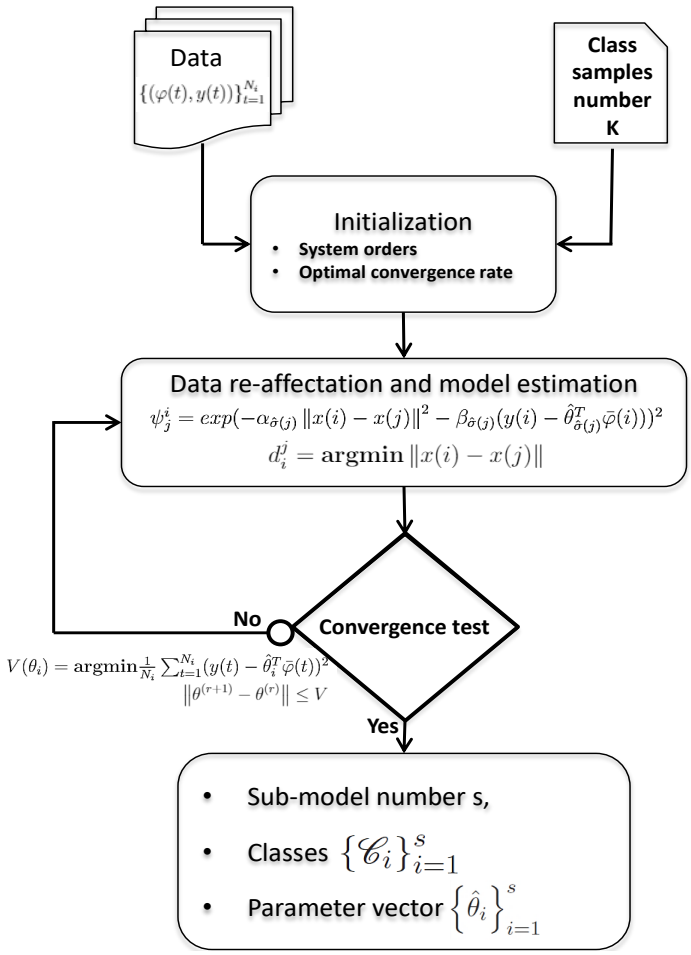

Figure 8: Parameter estimation and data classification algorithm

where $\bar{y}$ and $\hat{y}$ are respectively the mean and the estimate of the indoor temperature measurement $y(t)$.

3. Results

3.1. Systems description

The experimental study is carried out using a test cell equipped with renewable energy systems, mainly solar and geothermal. The cell is located at the Institute of Civil and Mechanical Engineering of the University of Sciences and Technology of Oran, Algeria, where the coordinates are: 35.65^oN, 0.62^oW, with a north-south orientation, as shown Figure 10. The test cell consists of two juxtaposed rooms of identical dimensions: $4.7 \times 3.7 \times 2.8m^3$. The physical properties of the materials constituting are presented in Table 1.

Several sensors were used to measure the outlet temperature of the solar thermal collector, the inlet temperature of the heating floor, the outlet temperature of the heating floor and the indoor (in the center of the room and at a height of 1.4m) and outdoor air temperatures. Figure 9 shows the positioning of the measurement sensors on both systems. Table 2 shows the characteristics of the measurement sensors used such as its measuring range and accuracy. During the experimentation the sampling time is one samples per hours. In other terms we collect 24 points by day for each measured parameter value.

3.2. Experimental setup

For 46 days from 1 January 2014, we monitored the climate conditions, solar collector temperature, outlet heating floor and indoor air temperature and humidity, as shown in Figure 11. The results show that the outside air temperature of the site varies between 5 and 20^oC. Regarding the humidity level, it grows up to 100%. Furthermore, the solar radiation received on the site is is around $2500W/m^2$. This power influences the thermal behaviour of the solar collector and the heating floor. Thus, if the solar radiation power received at the site raises, then the temperature of the output of the solar thermal collector also increases, which in turn increases the temperature of the floor heating system. The temperature of the solar thermal collector rises by 46^oC with a return temperature of the heating floor of 32^oC. The change in temperature at the output of the solar thermal collector affects the indoor air temperature. There are two parts in figure 11 (solar collector temperature and indoor air temperature curves), from

Composition	Thickness (m)	Conductivity (W/mK)	Density (kg/m^3)	Heat capacity (J/kgK)	Thermal transmittance (W/m^2)	Thermal resistance (m^2KW^{-1})
Vertical walls						
Cement plaster	0.01	1.5	1500	1000	15	0.0066
Wall first brick	0.1	0.476	690	900	4.76	0.21
Polystyrene Insulation	0.04	0.039	25	1380	1.21	0.82
Wall second brick	0.1	0.476	690	900	4.76	0.21
Cement plaster	0.01	1.5	1500	1000	15	0.0066
Ceiling						
Tightness and external mortar	0.05	0.04	1150	1000	0.8	1.25
Polystyrene insulation	0.04	0.039	25	1380	0.51	0.51
Compression slab	0.04	1.75	2300	1000	43.75	0.022
Hollow body	0.16	1.14	1850	1000	7.125	0.14
Plaster	0.02	0.42	1200	837	2.1	0.047
Floor heating						
Gerflex coating	0.003	0.31	1.046	1190	103.33	0.009
Concrete	0.1	1.75	0.92	2300	17.5	0.057
Cross-linked tube	18/20 $e.10^{-3}$					
Concrete	0.1	1.75	0.92	2300	17.5	0.057
Insulation	0.04	0.039	1.45	20	0.975	1.025

Table 1: Thermo-physical properties of the different material layers of the cell.

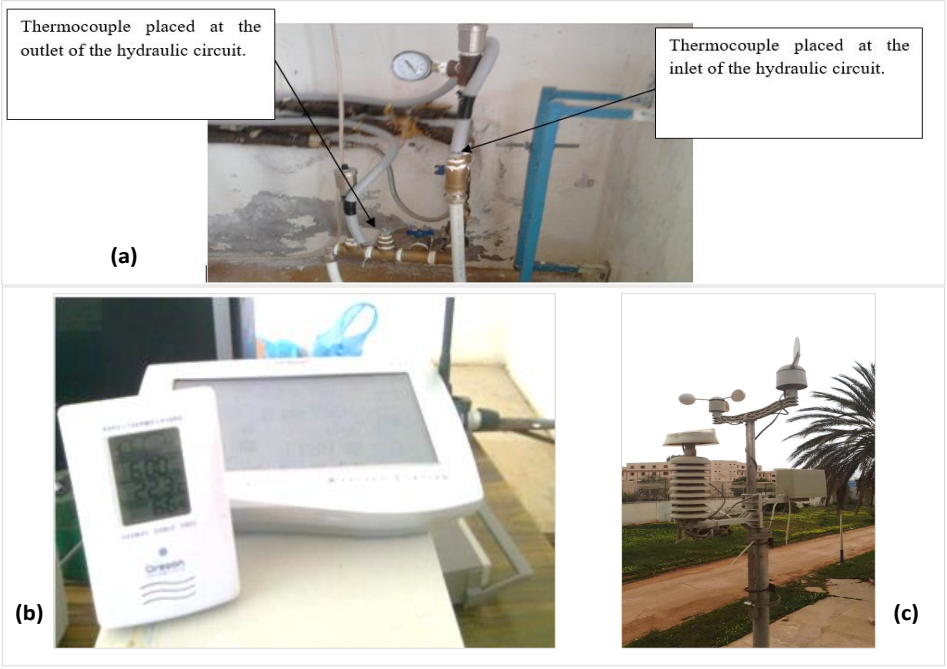

Figure 9: Measurement sensors [2]. (a) Inlet and outlet temperature. (b) Indoor humidity and temperature. (c) Weather station.

Figure 10: Experimental cell [2].

Measured parameter	Measuring range	Accuracy	Type of sensor	Units
Temperature	$-40^oC < T < +60^oC$	$\pm 1.5^oC$	Thermocouple	^oC
Outdoor temperature	$-40^oC < T < +60^oC$	$\pm 1^oC$	Weather station	^oC

Table 2: Wireless sensor characteristics

0 to 400 and from 400 to 1100. The indoor air temperature varies with the variation of the solar thermal collector. Starting to sample 400, the temperature of the solar collector rises. That leads to an increase in the indoor air temperature of up to 22°C. However, the hygrothermal behaviour of the indoor air remains within a thermal comfort range (Temperature: 17^oC - 22^oC, humidity: 40% - 60%).

Based on equation (9), we used the collected data (Figure 11) to estimate PWARX model parameters defined in equation (11) as well as the operating modes defined in equation (14). Therefore, the measured output is compared with the predicted output as shown in Figure 12 to verify the performance of the identified PWARX model.

3.3. Numerical results

This section presents a comparison between the data collected, the TRNSYS results and PWARX models. Figure 13 shows the comparison between the estimated switching evo-

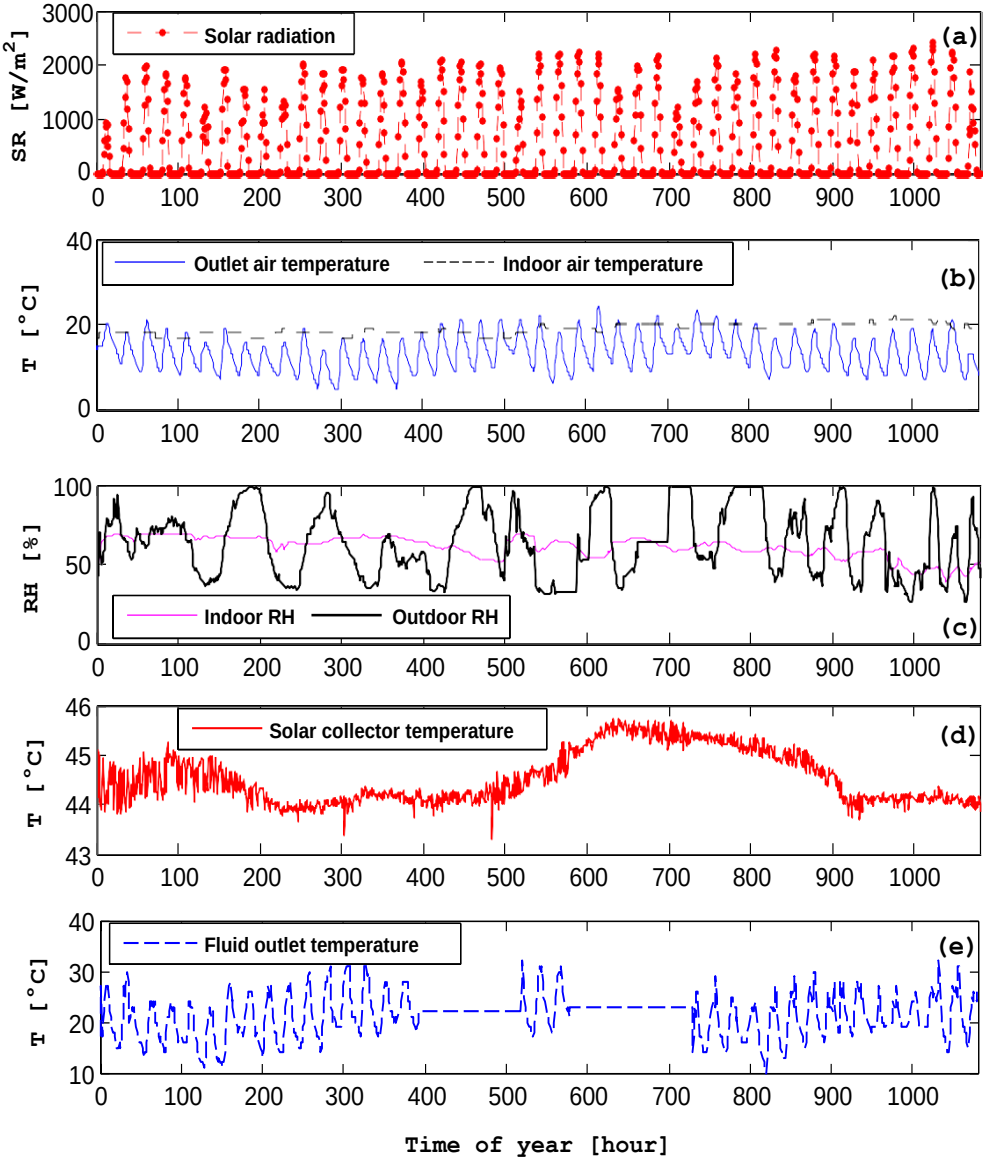

Figure 11: Experimental results: (a) Solar radiation, (b) Outdoor and indoor air temperature, (c) Outdoor and indoor humidity, (d) Solar collector fluid temperature, (e) Fluid outlet temperature of the floor heating.

lution of the operating modes (figure below) and pump operation (ON/OFF) according to a control system modelled on TRNSYS (Outlet flow rate). The Outlet flow data found by TRNSYS are used to train the PWARX model.

The algorithm estimates three (3) operating modes describing the thermal behaviour of the experimental cell heated by the DSF system (Figure 13, bottom part). However, we can distinguish two modes for TRNSYS: mode 1, where the pump system is ON and mode 2, where the pump system is OFF. Thus, we see that the discrete states change (i.e., operating modes) depending on the solar irradiation and the pump flow rate (TRNSYS). As a reminder, the pump operation is carried out in relation to the temperature differences DTU (Upper dead-band =5^oC) and DTL (Lower dead-band= 2^oC).

Looking at figures 13 and 14, we see that the first sub-model (first mode) corresponds to the case where the pump is ON or OFF with the presence of solar radiation (illuminated day). Thus, we can observe between 910 and 1110 samples (Figure 14) the case where solar radiation is present and pump is ON, and around 800 samples (Figure 13), for example, the case where the pump is OFF during the day. For the latter, this can be explained based on the outdoor air temperature and solar radiation. The algorithm has identified that mode 1 will appear during the day when the indoor environment is comfortable or when the pump needs to be activated to reach a comfortable level.

On the other hand, the second sub-model (resp. second operating mode) corresponds to the situation where the pump

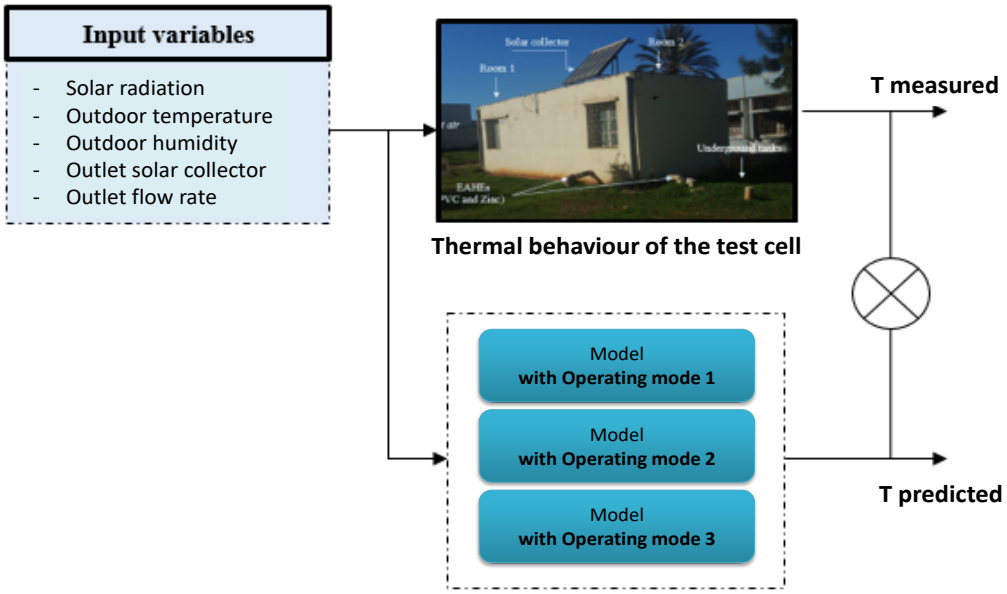

Figure 12: Thermal behaviour model identification

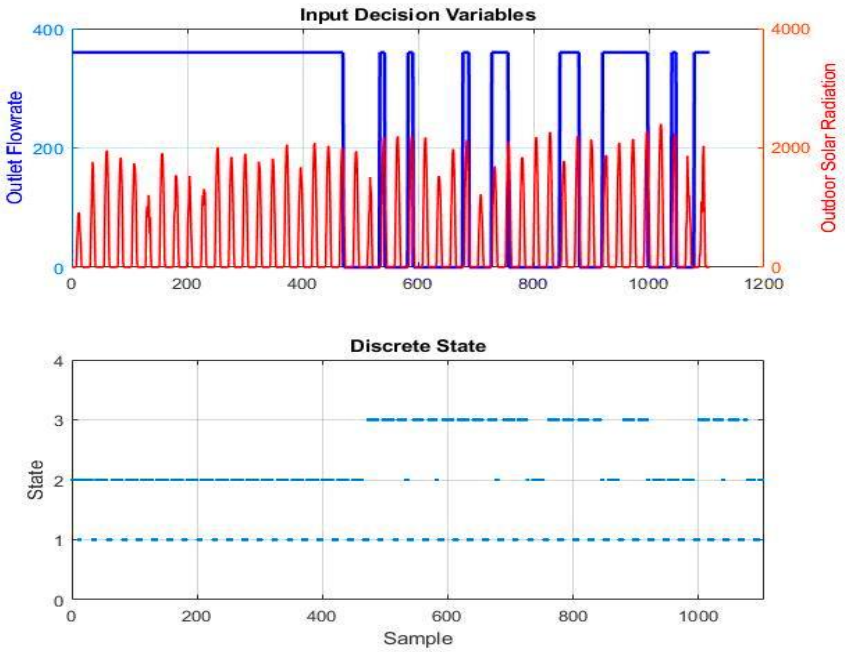

Figure 13: Operating mode identification

system is active (ON) and night. In this case, it is shown that during the night, when the internal temperature decreases, the pump is switched ON to supply the heating floor with heat from the solar thermal collector. The control was carried out in relation to a variation in temperature and not with day or night. As a result, the temperature at the output of the solar thermal collector is cold (at night), so the pump supplies the floor with a cold temperature. The thermal inertia of the floor did not play its role during the night for this period.

Finally, the third sub-model (resp. third operating mode) corresponds to the situation where the heating system is OFF and night (Figure 14). The pump has not been switched ON for this mode because the indoor air temperature corresponds to the requirements. For this case, the thermal inertia of the floor heats the requested interior ambience. It can be concluded that state 3 corresponds to the release of heat from the slab (thermal inertia) during the night. So the question is, why is state 3 only observed from 450 (Figure 13).

The floor heating system before sample number 450 was not thermally charged enough to release heat naturally at night

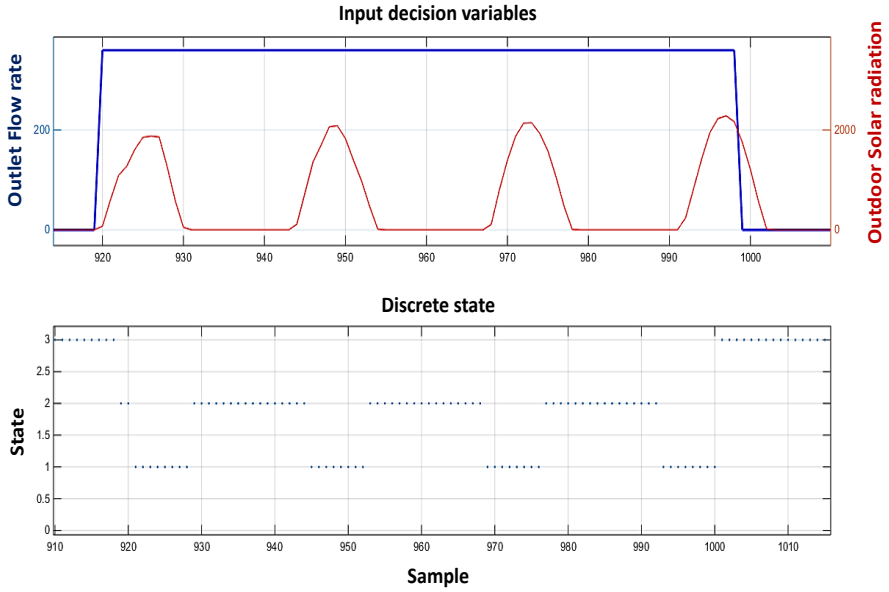

Figure 14: Switching rules associated to the thermal behaviour

(thermal inertia). This can be related to the solar collector temperature (Figure 11-(c)). From 400, the temperature of the solar collector rises, which increases the temperature of the floor, resulting then leads to an increase in heat storage in the slab. Once the slab is sufficiently loaded, heat will be naturally released during the night when the indoor air temperature drops. We thus note that it would be difficult to identify the period during which indoor air heating is achieved by thermal inertia through the TRNSYS model.

The description of each operating mode is summarized in Table 3 below.

According to Figure 15, we compute some numerical criterion to validate our model. With the FIT criterion, we also use typical fitting values as Root Mean Squared Error (RMSE), Mean Square Error (MSE) and Variance Accounted For (VAF) for our case. Each criterion is a statistical technique designed to find the "best fit" of one type of model to a particular system under investigation. For example, if the model matched the segment scores exactly, the MSE and RMSE values would be zero. However, the FIT and VAF values would be 100. So, by confronting with PWARX model, the TRNSYS model is less precise than the PWARX measurements (see Table 4).

Besides, with the PWARX model, it is straightforward to understand physical phenomena. As we can see, the PWARX-thermal model makes possible the understanding of system behaviour. Especially, the discrete state is not explained or well visualized in the white box such as TRNSYS. According to the indoor temperature estimation, Figure 15 (top part) compares 1100 samples. We observe that the indoor air temperature increases with the appearance of the third mode. That relates to the operating function of heat transfer by the thermal inert of the slab. During the same period, mode 2 (Pump ON and night) is not frequently active. The indoor environment is heated during the night by the thermal inertia (mode 3) and sometimes the pump is switched ON (mode 2) when the indoor air temperature drops, which is an unfavourable mode for indoor air temperature. For this purpose, it can be said that the PWARX model can be used to identify favourable and unfavourable system operation, which helps in diagnosing and decision support. For example, during the period where mode 2 is activated, it is proposed to switch OFF the pump and activate another auxiliary heating system in order to provide heating needs during the night. To this end, the model makes it possible to estimate the activation time of each operating mode as well as the energy consumed (for a pump power of 60W).

Figure 16 shows that for the total test period (1110hours) the worst mode (mode 2) lasts 454hours which results in an energy consumption of 27.24kWh. On the other hand, the thermal gain provided by thermal inertia (mode 3) is 18.6kWh during 310hours for the whole test period,which corresponds to 3.58hours per day.

4. Discussion

4.1. Summary of major findings and recommendations

In this study, we developed experimental and numerical studies of the thermal performance of the direct solar floor in the Algerian context. In the same view and context, several studies were conducted on the simulation of the thermal behaviour of the DSF using white-box models such as [23] and [9] who have used TRNSYS tools and Matlab Simulink.

Our research strategy shows the advantage of the predictive model (PWARX) to simulate and understand the thermal behaviour of the DSF system. Thermal solar energy storage is one of the promising techniques that has not yet been widely developed in northern Algeria. Thus, according to the results found, the DSF can provide thermal comfort for the climatic

Modes	Solar radiation	Pump operation
Mode 1	Presence of solar radiation	Pump system is ON or OFF
Mode 2 (heating needs)	Night	Pump system in ON
Mode 3 (thermal inertia)	Night	Pump system is OFF

Table 3: Identified operating mode

Model Criterion	FIT [%]	MSE	RMSE	VAF [%]
PWARX	54.32	0.308	0.555	81.51
TRNSYS	5.54	1.64	1.28	8.76

Table 4: Model comparison and validation

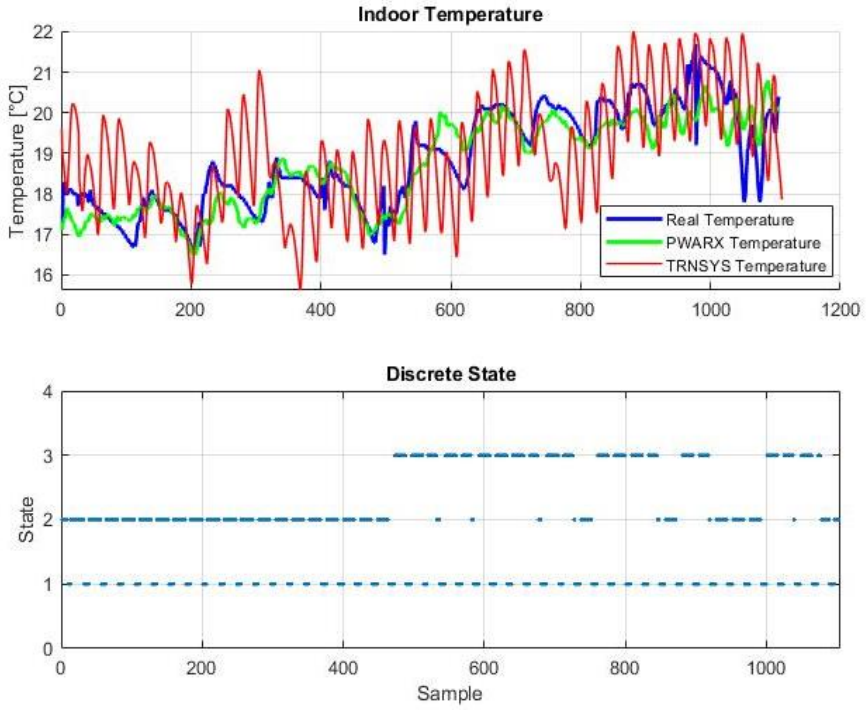

Figure 15: Indoor air temperature validation and operating modes

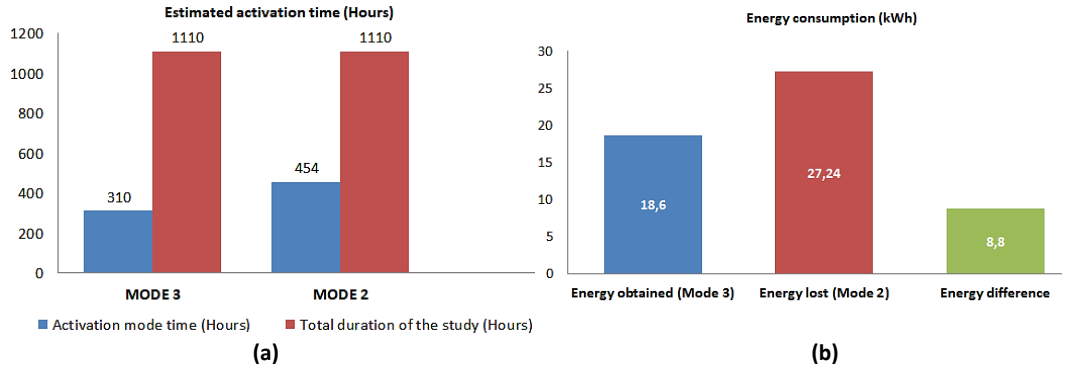

Figure 16: Activation time and energy consumption for both mode 2 and 3. (a) Activation time. (b) Energy provided.

conditions of the Oran city (northern Algeria). The most important and tangible results of our application are listed as follows:

- The hydrothermal behaviour of the indoor air remains

within a thermal comfort range (Temperature: 17°C - 22°C, humidity: 40% - 60%).

- The temperature of the solar thermal collector can be as high as 46°C.
- The comparison between TRNSYS, PWARX and experimental data shows that the proposed model ensures a good validation.
- Three operating modes have been generated by the PWARX model instead of two for TRNSYS (ON or OFF pump operation).
- For the night, two modes have been identified: mode 2 corresponds to the situation where the pump system is (ON) which is due to the drop in internal temperature, and mode 3 corresponds to the situation where the interior environment is heated by the thermal inertia of the slab. The first mode, which corresponds to the case of the pump system is (ON) during the day.
- The model evaluated the duration and the energy provided by the thermal inertia which is estimated at 310 hours (An average of 3.58hours per day) and 18.6kWh for a test period of 1110hours.

4.2. Study strength and limitations

In this study, a new concept to predict the "true" thermal behaviour of a DSF system, evolving in the Algerian climate, is addressed. That is possible because we compute the numerical model with data collected from the system investigated. Indeed, data-driven approaches are well recognized for their outstanding performances to describe the behaviour of a system. That will be performed without any physical knowledge, in contrast to what is implemented into TRNSYS or ENERGYPLUS. Accordingly, they can simplify the understanding of the thermal behaviour of the DSF system.

Furthermore, the approaches allow us to realize a diagnosis according to the system functioning. In other terms, identify, for instance, favourable and unfavourable modes. For our case, this model makes it possible to identify the moment of natural operation of the slab by thermal inertia. From our best knowledge, this is a thing that not feasible with models proposed in the literature. Therefore, we believe that the concept can help civil engineers to make a quick diagnosis of the system and predict the "true" thermal behaviour with a minimum of inputs.

We could therefore spread the experiment to other locations with a Mediterranean climate, to mention just a few examples: North Africa, Southern Europe (France, Italy, Spain etc.) and Western Asia. In Figure 17, we present an overview of the various world areas with the same climate, to which the system proposed, in this paper, can be referenced. However, the thermal behaviour of the DSF changes according to the solar deposit. In other terms, if the system is installed away from the Mediterranean climate, then its performance could change.

Finally, the paper proposes a new application for building heating system. It could consider as a "new" contribution to the literature and the field of civil engineering. Nevertheless, we are aware that our study has limitations as any other. The experimental test has been achieved for just one month. The measurement campaign could have benefited from a more prolonged monitoring period covering the whole winter season. We notice, however, that our study has been handled using the most appropriate data.

4.3. Implications on practice and future research

The purpose of these results showed the importance of direct solar floor application for the Mediterranean climate to cover heating needs. Moreover, this study provides for building thermal engineers with information on the functioning of such a system based on a new data-driven model. That allows them to thoroughly undertake the implementation of the system, whether it is performed in the Mediterranean climate in general or in Algeria in particular.

The proposed model allows a quick diagnosis for building thermal engineers to identify the different operating modes and estimate the thermal and energy gain brought by the inertia of the slab. With this diagnosis, they will be able to dimension well the DSF (solar collector and slab) for different climates. Another important implication of our study is that it calls for the valorization of the solar deposit, which has Algeria in particular and Mediterranean cities worldwide to replace the conventional heating system such as the boiler. We find it essential that the National Building Efficiency Standard of Algeria use our findings to improve the thermal regulation, which is under development. This case study should investigate real-time building energy management method that predicts heat transfer through DSF and suggest adaptation strategies following building operators and occupants. Meanwhile, governments and green building councils should promote exemplary building design in Mediterranean climates with DSF systems and the switching-linear model for heat management.

Another complex operating mode that could be obtained in the DSF system is the integration of phase change material (PCM) in the slab. Considering the phase change of the PCM and the dephasing of the thermal inertia concurrently is a complex thermal phenome that is difficult to detect by physical models. The subsequent step for our research project is to integrate the PCM in the slab and test the developed model to identify, for instance, the fourth operating mode according to the phase change of the PCM.

5. Conclusion

We investigate in this paper the heating performance of a direct solar floor system coupled with an experimental cell and evolving under Mediterranean climate. The study has been done for 45 days during the winter period. Accordingly, we use data collected from the system to estimate and validate the proposed switching linear model for the DSF system. The literature review indicates a knowledge gap that must be filled. Also, none of the published studies addressed the following issues:

Figure 17: Mediterranean climate covering different geographical regions of the world (Modified from [17])

- Numerical study of the effect of the slab thermal inertia on the energy performance of the DSF;
- Identify when the DSF slab generated heat through thermal inertia at night;
- Detect the different operation modes of the DSF and identify the unfavourable and favourable modes for the system;
- Assessing heating time through thermal inertia;
- Assessing the energy gain provided by thermal inertia.

So, the methodology has been presented in this paper, and we also show how it can explain the "true" thermal behaviour of the system and generate its operating condition. From this study, we identify three operating modes. It corresponds to the operation of the system during the day and at night. During the night-time, two modes are defined. One of which corresponds to the moment where the heating system is applied. The results show that the direct solar floor provides thermal comfort for the Mediterranean climate. The indoor air hygrothermal behaviour remains within a thermal comfort range (Temperature: 17°C - 22°C, humidity: 40% - 60%).

On the other hand, the proposed model makes it possible to diagnose the system functioning and identify the modes where the performance is the best (resp. worst). Herein, it has been shown that mode 2 is the most unfavourable mode regarding thermal performance, with an energy consumption of 27.24kWh. This heating requirement corresponds to the case when thermal inertia does not play its role during the night. For this case, it is proposed to switch OFF the DSF and activate another auxiliary heating system in order to provide heating needs during the night. However, mode 3 can be seen as a good performance. It corresponds to the thermal inertia heating which lasted 310hours for the whole test period, which corresponds to an average of 3.58hours per day and allowed us to save 18kWh of energy.

Acknowledgements The authors thank Maaden HAFSA, assistant professor at the University of Oran, for the solar radiation data.

References

[1] APRUE. La consommation énergétique finale. Technical report, APRUE.ORG, http://www.aprue.org.dz/documents/, 2017.

[2] M. H. Benzaama. *Etude du confort thermique dans l'habitat par des procédés géo-héliothermiques*. Université de Reims - Université de Sidi Bel Abbes, Thèse de Doctorat, 2017.

[3] M. H. Benzaama, L. H. Rajaoarisoa, B. Ajib, and S. Lecoeuche. A data-driven methodology to predict thermal behavior of residential buildings using piecewise linear models. *Journal of Building Engineering*, 32:101523, 2020.

[4] D.Abbaz and A.Chaker. The effect of the thermal inertia on the temperature of a heating slab. *Sciences & Technology*, 3:13–16, 2018.

[5] J. Feng, F. Bauman, and S. Schiavon. Experimental comparison of zone cooling load between radiant and air systems. *Energy and buildings*, 84:152–159, 2014.

[6] M. S. Karimi, F. Fazelpour, M. A. Rosen, and M. Shams. Comparative study of solar-powered underfloor heating system performance in distinctive climates. *Renewable Energy*, 130:524–535, 2019.

[7] P. Kattan, K. Ghalia, and M. Al-Hindi. Modeling of under-floor heating systems: a compromise between accuracy and complexity. *http://doi.org/10.1080/10789669.2012.649881*, 18:468–480, 2012.

[8] H. Kazeoui, R. Belarbi, A. Tahakourt, and A. Ait-Mokhtar. Energy performance evaluation of direct solar floor in traditional and modern buildings. *Building Services Engineering Research and Technology*, pages 1–18, 2015.

[9] M. C. Lekhal, R. Belarbi, A. M. Mokhtari, M. H. Benzaama, and R. Bennacer. Thermal performance of a residential house equipped with a combined system: A direct solar floor and an earth–air heat exchanger. *Sustainable Cities and Society*, 40:534–545, 2018.

[10] Y. Liu, D. Wang, and J. Liu. Study on heat transfer process for in-slab heating floor. *Building and Environment*, 54:77–85, 2012.

[11] S. Lu, Y. Zhao, K. Fang, Y. Li, and P. Sun. Establishment and experimental verification of trnsys model for pcm floor coupled with solar water heating system. *Energy and Buildings*, 2017.

[12] M. Mehdaoui, A. Hazami, A. Messaouda, and A. Guizani. Performance analysis of two types of solar heating systems used in buildings under typical north-african climate (tunisia). *Appl. Therm. Eng.*, 165:114203, June 2020.

[13] S. Menhoudj, D. Sifodil, and A. Mokhtari. Etude expérimentale d'un système solaire actif -psd. *Revue des énergies renouvelables du CDER*, 15(03):479–488, 2012.

[14] A. Odyjas and A. Gorka. Simulations of floor cooling system capacity. *Applied Thermal Engineering*, 51:84–90, 2015.

[15] D. Olsthoorn, F. Haghighat, A. Moreau, and G. Lacroix. Abilities and limitations of thermal mass activation for thermal comfort, peak shifting and shaving: A review. *Building and Environment*, 118:113–127, 2018.

[16] P. Papillon. *Contribution à l'amélioration de la technique du plancher*

solaire direct, Analyse de la solution dalles minces et gestion optimisée du chauffage d'appoint. Université de Savoie, Thèse de Doctorat, 1992.

[17] M. C. Peel, B. L. Finlayson, and T. A. McMahon. Updated world map of the köppen-geiger climate classification. *Hydrology and Earth System Sciences*, 11(5):1633–1644, 2007.

[18] K.-N. Rhee and K. Kim. A 50 year review of basic and applied research in radiant heating and cooling systems for the built environment. *Building and Environment*, 91:166–190, 2015.

[19] E. Shaviv, A. Yezioro, and I. Capeluto. Thermal mass and night ventilation as passive cooling design strategy. *Renewable Energy*, 24:445–452, 2001.

[20] I. Sobhy, A. Brakez, and B. Benhamou. Energy performance and economic study of a solar floor heating system for a hammam. *Energy and Buildings*, 141:247—-261, 2012.

[21] S. Verbeke and A. Audenaert. Thermal inertia in buildings: A review of impacts across climate and building use. *Renewable and Sustainable Energy Reviews*, 82:2300–2318, 2018.

[22] H. Wang and H. Meng. Improved thermal transient modeling with new 3-order numerical solution for a district heating network with consideration of the pipe wall's thermal inertia. *Energy*, 160:171–183, 2018.

[23] F. Yang, J. Liu, Q. Sun, L. Cheng, and R. Wennersten. Simulation analysis of household solar assistant radiant floor heating system in cold area. *Energy Procedia*, 158:631—-636, 2019.

[24] Q. Zhu, X. Xu, J. Wang, and F. Xiao. Development of dynamic simplified thermal models of active pipe-embedded building envelopes using genetic algorithm. *International Journal of Thermal Sciences*, 76:258–272, 2014.